Bose-Einstein Condensation of Chromium

Axel Griesmaier,* Jörg Werner, Sven Hensler, Jürgen Stuhler, and Tilman Pfau

5. Physikalisches Institut,† Universität Stuttgart, 70550 Stuttgart, Germany

(Received 1 March 2005; published 29 April 2005)

We report on the generation of a Bose-Einstein condensate in a gas of chromium atoms, which have an exceptionally large magnetic dipole moment and therefore underlie anisotropic long-range interactions. The preparation of the chromium condensate requires novel cooling strategies that are adapted to its special electronic and magnetic properties. The final step to reach quantum degeneracy is forced evaporative cooling of ^{52}Cr atoms within a crossed optical dipole trap. At a critical temperature of $T_c \approx 700$ nK, we observe Bose-Einstein condensation by the appearance of a two-component velocity distribution. We are able to produce almost pure condensates with more than 50 000 condensed ^{52}Cr atoms.

DOI: 10.1103/PhysRevLett.94.160401 PACS numbers: 03.75.Hh

The essential properties of degenerate quantum gases depend on range, strength, and symmetry of the interactions present. Since the first observation of Bose-Einstein condensation in weakly interacting atomic gases, eight different elements have been Bose-Einstein condensed [1–9]. All these elements, mainly alkali atoms, interact dominantly via short-range isotropic potentials. Based on this effective contact interaction, many exciting nonlinear phenomena have been studied [10,11]. Bose-Einstein condensates (BECs) with contact interaction have also been used to investigate solid-state physics problems such as the Mott-metal-insulator transition [12,13]. Tuning the contact interaction, the collapse and explosion (''Bosenova'') of Bose-Einstein condensates has been studied [14] and new types of quantum matter such as a Tonks-Girardeau gas have been realized [15]. In a chromium Bose-Einstein condensate, one can not only tune the short-range contact interaction using one of the recently observed Feshbach resonances [16] but can also investigate the effects of the long-range and anisotropic dipole-dipole interaction. This becomes possible because, compared to other Bose-condensed elements, the transition metal chromium has a unique electronic structure. The valence shell of its ground state contains six electrons with parallel spin alignment (electronic configuration: $[\mathrm{Ar}]3d^5 4s^1$). For the bosonic chromium isotopes, which have no nuclear spin, this gives rise to a total electronic spin quantum number of 3 and a very high magnetic moment of $6\mu_B$ (μ_B is the Bohr magneton) in its ground state $^7S_3$. Since the magnetic dipole-dipole interaction (MDDI) scales with the square of the magnetic moment, it is a factor of 36 higher for chromium than for alkali atoms. For this reason, dipole-dipole interactions which have not yet been investigated experimentally in degenerate quantum gases will become observable in chromium BEC. For example, it was shown in [17] that the MDDI in chromium is strong enough to manifest itself in a well pronounced modification of the condensate expansion that depends on the orientation of the magnetic moments. Tuning the contact interaction between ^{52}Cr atoms close to zero will allow one to realize a dipolar BEC [18] in which the MDDI is the dominant interaction. In this way, many predicted dipole-dipole phenomena can be investigated experimentally. These include the occurrence of a Maxon-Roton in the excitation spectrum of a dipolar BEC [19] or new kinds of quantum phase transitions [20,21] as well as the stability and the ground state of dipolar BECs [22–24] can be investigated experimentally. Since also the MDDI is tunable [25], a degenerate quantum gas with adjustable long- and short-range interactions can be realized.

A chromium BEC is also unique with respect to the technical applications of degenerate quantum gases. As a standard mask material in lithographic processes, chromium is a well suited element for atom lithography [26]. It has already been used to grow nanostructures on substrates by direct deposition of laser-focused thermal atomic beams. Furthermore, structured doping has been demonstrated by simultaneously depositing a homogeneous matrix material and laser-focused chromium [27]. Performing the step from incoherent thermal atomic beams to coherent atom sources (BECs) promises to increase the potential of atom lithography, much as the invention of the laser did in classical optical lithography.

Our preparation scheme combines magneto-optical, magnetic, and optical trapping techniques. It requires novel cooling strategies that are adapted to the special electronic and magnetic properties and to the need to circumvent relaxation processes originating from the dipolar character of the atoms. A beam of chromium atoms is generated by a high temperature effusion cell at 1600 °C and slowed down by a Zeeman slower. Using a continuous loading scheme [28] followed by an in-trap Doppler-cooling stage [29], we prepare $\sim 1.3 \times 10^8$ atoms in the energetically highest projection $m_J = +3$ of the $^7S_3$ ground state in a Ioffe-Pritchard trap. Subsequently, during 13 s of radiofrequency (rf) induced evaporation, the atoms are cooled in the magnetic trap to a phase space density 5 orders of magnitude less than degeneracy. The extraordinarily large magnetic dipole moment of chromium leads to increasing two-body loss in the form of dipolar relaxation [30] with

increasing spacial density of the cloud. This causes rf-evaporation to become inefficient and prevents ^{52}Cr from reaching the regime of quantum degeneracy in a magnetic trap. To overcome this loss mechanism, the atoms have to be transferred into the energetically lowest Zeeman substate $m_J = -3$. In this state, energy conservation suppresses dipolar relaxation if the Zeeman splitting is much larger than the thermal energy of the atoms. As chromium atoms in states $m_J < 0$ are repelled from regions with low magnetic fields, these atoms cannot be trapped magnetically. We therefore adiabatically transfer about 40% of the atoms into an optical dipole trap where the trapping forces are independent of the Zeeman substate. The optical trapping potential is formed by two beams produced by a 20 W fiber laser at 1064 nm. The stronger horizontal trapping beam has a waist of 30 μm and a power of up to ~9 W. The symmetry axis of the trapping potential formed by this beam coincides with the axis of our magnetic trap to achieve the largest overlap between the two trap volumes for efficient transfer into the optical trap. Ramping up this beam to its maximum intensity during the final step of the rf ramp, we are able to transfer 1.8×10^6 atoms into the optical trap.

The trap has a depth of 130 μK and trap frequencies of 1450 and 12 Hz in the radial and axial directions. After switching off the magnetic trapping potential, we optically pump the atoms to the $m_J = -3$ state using a laser resonant to the $^7S_3 \rightarrow {}^7P_3$ transition at an offset field of 9 G in the vertical direction. In contrast to commonly used rf techniques, this optical technique has the advantage that the occupation numbers of the Zeeman substates are not only inverted but the polarization is also purified. This is necessary in our experiment because in the magnetic trap all low-field seeking states are occupied due to dipolar relaxation. The efficiency of the transfer is close to 100% and is reflected in a dramatic increase of the lifetime of the trapped gas from 6 s in the $m_J = +3$ state to >140 s in the $m_J = -3$ state as shown in Fig. 1. During all further steps of preparation, the offset field is kept on in order to prevent thermal redistribution among the other Zeeman states.

The optical transfer is followed by a 5 s stage of plain evaporation during which the number of atoms in the trap drops by 50% and the phase space density increases to $\sim 10^{-2}$. This effect becomes visible in a decrease of the axial size of the expanded cloud with increasing holding times in the trap (see the inset of Fig. 1). To increase the local density and the elastic collision rate for evaporative cooling, a second beam in the vertical direction with a waist of 50 μm and a power of ~4.5 W is additionally ramped up adiabatically within the first 5 s in the optical trap. After the intensity of the horizontal beam is reduced to 70% of its initial value within 10 s, about 300 000 atoms are trapped in this crossed trap. Forced evaporation towards the critical temperature for the condensation proceeds now by gradually reducing the intensity of the

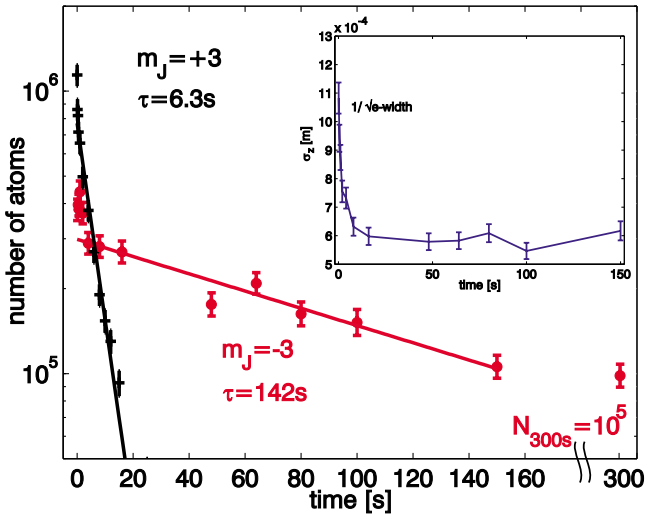

FIG. 1 (color online). Comparison of trap lifetimes before (crosses) and after (circles) pumping the atoms to the lowest Zeeman substate. The inset shows the change of the axial size of the expanded cloud in time of flight after different holding times.

horizontal beam over 11 s. Degeneracy is reached at a remaining power of ~800 mW in the horizontal beam. After holding the atoms in the final trapping potential for 25 ms, we switch off both beams simultaneously and let the cloud expand freely for a variable time of flight. The cloud is then detected using a standard absorption imaging technique with a resonant probe beam propagating in the horizontal direction, perpendicular to both trapping beams.

The onset of quantum degeneracy becomes visible in absorption images of the relaxed chromium cloud. Figure 2 shows the profiles of the cloud after 5 ms of free expansion at different final powers of the horizontal trapping beam before releasing the cloud. Figure 2(a) displays the situation at a final power of 1.4 W. The cloud has the Gaussian profile of a pure thermal distribution corresponding to a temperature of ~1.1 μK, very close to the critical temperature T_C. In Fig. 2(b), the cloud was released from a trap with a final power of 650 mW in the horizontal beam. The two-component distribution indicates the presence of a Bose-Einstein condensate. The temperature of the remaining thermal part of the cloud is 625 nK. Reducing the laser power even further to ~370 mW leaves an almost pure condensate with more than 50 000 atoms and a non-Gaussian distribution as depicted in Fig. 2(c). At the end of our evaporation ramp, the trap frequencies in the visible axes are nearly equal. As expected, the expansion of the condensate is almost isotropic and the aspect ratio of the expanded condensate stays constant at ~1.

A series of images of such a condensate taken after variable expansion times between 1 and 9 ms is shown in Fig. 3(a). The situation is different if the BEC is released from an anisotropic trapping potential. The images in Fig. 3(b) show the expansion of the condensate for the

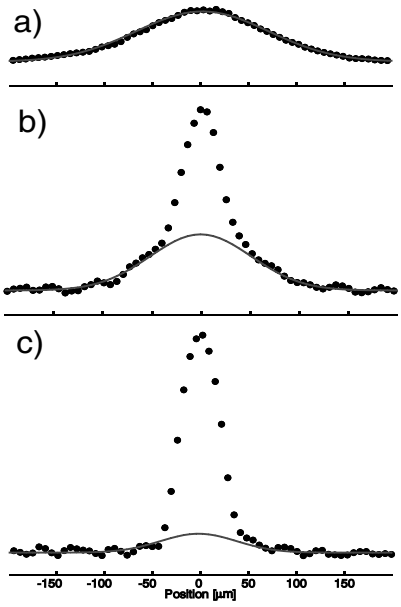

FIG. 2. Density profiles from absorption images of atom clouds taken after 5 ms of ballistic expansion: (a) thermal cloud at 1.1 μK; (b) two-component distribution at 625 nK, slightly below T_C; (c) nearly pure condensate with 47 000 atoms.

same time of flight series as before, but from a trap with a $\sim$20 times higher intensity in the horizontal beam. In this case the BEC was prepared in the same way as in Fig. 3(a) except that the trapping potential was deformed by adiabatically increasing the horizontal laser power within 250 ms after the formation of the BEC. The series shows a clearly anisotropic expansion of the cloud. From a cigar shaped trap in the horizontal direction, the aspect ratio changes in time of flight to elongated in the vertical direction. To show the critical behavior at the point of emerging degeneracy, we determine the number of atoms in the condensate and the thermal fraction separately. We extract these numbers by fitting a two-component distribution function to the density profiles of the clouds at different final laser powers.

In Fig. 4, the fraction of condensed atoms in the total number of atoms (N_0/N) is plotted versus the ratio of the temperature of the remaining thermal part to the critical temperature (T/T_C). When we approach the critical temperature from above ($T/T_C > 1$), the kink in the condensate fraction plot marks the onset of Bose-Einstein condensation and provides an experimental value for the critical temperature of $T_{\mathrm{exp}} \sim 700$ nK. Based on the trap frequencies, the number of atoms, and the temperature, we have also calculated the expected condensate fraction for an ideal gas following the equation

$$\frac{N_0}{N} = 1 - \left(\frac{T}{T_C}\right)^3 \tag{1}$$

with

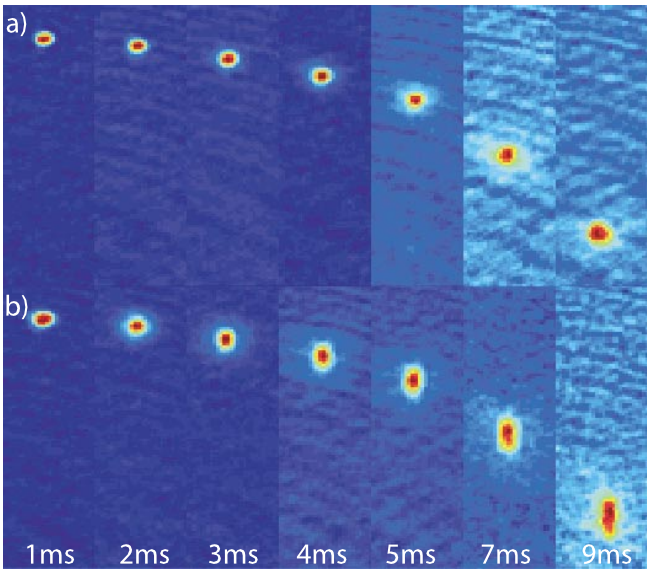

FIG. 3 (color). Time of flight series of absorption images with expansion times from 1 to 9 ms. (a) BEC released from an almost isotropic trap; (b) BEC released from an anisotropic trap.

$$T_C^0 \approx 0.94 \frac{\hbar\omega}{k_B} N^{1/3} \tag{2}$$

being the critical temperature. When finite size effects as well as a correction arising from the contact interaction [31] are taken into account, the critical temperature is shifted to lower temperatures:

$$T_C = T_C^0 + \delta T_C^{\mathrm{int}} + \delta T_C^{\mathrm{fs}} \tag{3}$$

where $\delta T_C^{\mathrm{fs}} = -0.73 \frac{\bar{\omega}}{\omega} N^{-1/3} T_C^0$ is a shift in the critical temperature due to the finite number of atoms and $\delta T_C^{\mathrm{int}} = -1.33 \frac{a}{a_{\mathrm{HO}}} N^{1/6} T_C^0$ takes into account the contact interaction. Here $a = 105 a_0$ is the chromium scattering length [16], a_0 being Bohr's radius, a_{HO} is the harmonic oscillator length, T is the temperature of the thermal cloud, ω is the geometric, and $\bar{\omega}$ is the arithmetic mean of the trap frequencies. These expected values are represented by black dots in Fig. 4 and demonstrate a good agreement of our data with the predicted dependence.

In conclusion, we have demonstrated Bose-Einstein condensation of chromium atoms. We produce condensates with more than 50 000 chromium atoms, which is a very good basis for a series of promising experiments on the dipolar character of this novel quantum gas. We expect that both long- and short-range interaction can be tuned by magnetic fields. As chromium is a standard material in atom lithography, we also expect that an atom laser of chromium will have applications in lithography, possibly even enabling controlled deposition of single atoms.

We thank all members of our atom optics group for their encouragement and practical help. We acknowledge especially the contributions of Piet Schmidt and Axel Görlitz at

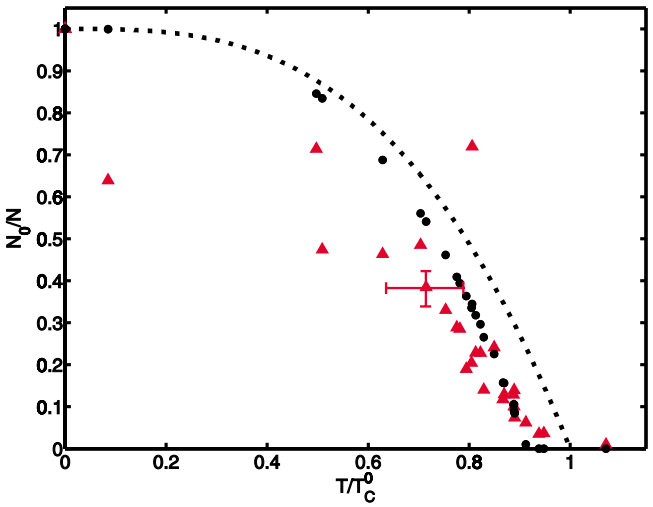

FIG. 4 (color online). Condensate fraction (N_0/N) dependence on temperature relative to the transition temperature of an ideal gas (T/T_C^0) given by Eq. (1). Triangles represent our measured data. Black circles represent the predicted fraction following Eq. (3) including corrections due to finite size effects and the contact interaction The dashed curve shows the dependence for the ideal gas. Error bars are mainly due to uncertainties in the measurement of the trap frequencies, the temperature, and the number of atoms.

earlier stages of the experiment. We thank Luis Santos, Paolo Pedri, Stefano Giovanazzi, and Andrea Simoni for stimulating discussions. This work was supported by the SPP1116 of the German Science Foundation (DFG).

*Electronic address: a.griesmaier@physik.uni-stuttgart.de
†http://www.physik.uni-stuttgart.de/institute/pi/5

[1] M. H. Anderson, J. R. Ensher, M. R. Matthews, C. E. Wieman, and E. A. Cornell, Science **269**, 198 (1995).
[2] K. B. Davis, M.-O. Mewes, M. R. Andrews, N. J. van Druten, D. S. Durfee, D. M. Kurn, and W. Ketterle, Phys. Rev. Lett. **75**, 3969 (1995).
[3] C. C. Bradley, C. A. Sackett, J. J. Tollett, and R. G. Hulet, Phys. Rev. Lett. **75**, 1687 (1995).
[4] D. G. Fried, T. C. Killian, L. Willmann, D. Landhuis, S. C. Moss, D. Kleppner, and T. J. Greytak, Phys. Rev. Lett. **81**, 3811 (1998).
[5] G. Modugno, G. Ferrari, G. Roati, R. J. Brecha, A. Simoni, and M. Inguscio, Science **294**, 1320 (2001).
[6] A. Robert, O. Sirjean, A. Browaeys, J. Poupard, S. Nowak, D. Boiron, and C. W. A. Aspect, Science **292**, 461 (2001).
[7] F. PereiraDosSantos, J. Léonard, J. Wang, C. J. Barrelet, F. Perales, E. Rasel, C. S. Unnikrishnan, M. Leduc, and C. Cohen-Tannoudji, Phys. Rev. Lett. **86**, 3459 (2001).
[8] T. Weber, J. Herbig, M. Mark, H.-C. Nägerl, and R. Grimm, Science **299**, 232 (2003).
[9] Y. Takasu, K. Maki, K. Komori, T. Takano, K. Honda, M. Kumakura, T. Yabuzaki, and Y. Takahashi, Phys. Rev. Lett. **91**, 040404 (2003).
[10] M. Weidemüller and C. Zimmermann, *Interactions in Ultracold Gases* (Wiley-VCH Verlag GmbH, Berlin, 2003), and references therein.
[11] J. R. Anglin and W. Ketterle, Nature (London) **416**, 211 (2002), and references therein.
[12] M. Greiner, O. Mandel, T. Esslinger, T. Hänsch, and I. Bloch, Nature (London) **415**, 39 (2002).
[13] T. Stöferle, H. Moritz, C. Schori, M. Köhl, and T. Esslinger, Phys. Rev. Lett. **92**, 130403 (2004).
[14] E. A. Donley, N. R. Claussen, S. L. Cornish, J. L. Roberts, E. A. Cornell, and C. E. Wieman, Nature (London) **412**, 295 (2001).
[15] B. Paredes, A. Widera, V. Murg, O. Mandel, S. Fölling, I. Cirac, G. V. Shlyapnikov, T. W. Hänsch, and I. Bloch, Nature (London) **429**, 277 (2004).
[16] J. Werner, A. Griesmaier, S. Hensler, A. Simoni, E. Tiesinga, J. Stuhler, and T. Pfau, cond-mat/0412049.
[17] S. Giovanazzi, A. Görlitz, and T. Pfau, J. Opt. B **5**, S208 (2003).
[18] M. Baranov, L. Dobrek, K. Góral, L. Santos, and M. Lewenstein, Phys. Scr. **T102**, 74 (2002), and references therein.
[19] L. Santos, G. V. Shlyapnikov, and M. Lewenstein, Phys. Rev. Lett. **90**, 250403 (2003).
[20] K. Góral, L. Santos, and M. Lewenstein, Phys. Rev. Lett. **88**, 170406 (2002).
[21] S. Yi, L. You, and H. Pu, Phys. Rev. Lett. **93**, 040403 (2004).
[22] D. H. J. O'Dell, S. Giovanazzi, and C. Eberlein, Phys. Rev. Lett. **92**, 250401 (2004).
[23] K. Góral and L. Santos, Phys. Rev. A **66**, 023613 (2002).
[24] L. Santos, G. V. Shlyapnikov, P. Zoller, and M. Lewenstein, Phys. Rev. Lett. **85**, 1791 (2000).
[25] S. Giovanazzi, A. Görlitz, and T. Pfau, Phys. Rev. Lett. **89**, 130401 (2002).
[26] M. Oberthaler and T. Pfau, J. Phys. Condens. Matter **15**, R233 (2003), and references therein.
[27] T. Schulze, T. Müther, D. Jürgens, B. Brezger, M. Oberthaler, B. Brezger, T. Pfau, and J. Mlynek, Appl. Phys. Lett. **78**, 1781 (2001).
[28] P. O. Schmidt, S. Hensler, J. Werner, T. Binhammer, A. Görlitz, and T. Pfau, J. Opt. B **5**, S170 (2003).
[29] P. O. Schmidt, S. Hensler, J. Werner, T. Binhammer, A. Görlitz, and T. Pfau, J. Opt. Soc. Am. B **20**, 960 (2003).
[30] S. Hensler, J. Werner, A. Griesmaier, P. O. Schmidt, A. Görlitz, T. Pfau, and K. R. S. Giovanazzi, Appl. Phys. B **77**, 765 (2003).
[31] S. Giorgini, L. P. Pitaevskii, and S. Stringari, Phys. Rev. A **54**, R4633 (1996).